Hindawi
Shock and Vibration
Volume 2021, Article ID 5020779, 11 pages
https://doi.org/10.1155/2021/5020779

Research Article

Model of Seismic Wave Field Excited by Horizontally Distributed Charge

Xu Qian and Wang Zhong-Qi

State Key Laboratory of Explosion Science and Technology, Beijing Institute of Technology, 100081 Beijing, China

Correspondence should be addressed to Xu Qian; chinaxuqian@126.com

Received 21 April 2021; Accepted 20 May 2021; Published 11 June 2021

Academic Editor: Yun Lin

The amplitude-frequency characteristics of seismic wave field excited by an explosive source can directly affect the accuracy of seismic prospecting. To reveal the laws by which the horizontally distributed charge excites the amplitude-frequency characteristics, a method to calculate seismic wave field excited by horizontally distributed charge was studied in this paper. By taking the spherical cavity source model as the basis, the superposition method was applied to obtain the approach of calculating seismic wave field excited by horizontally distributed charge. Compared with numerical simulation, the error of this method was controlled under 7%. As a matter of fact, the distributive charge can effectively reduce the impact on ground vibration and increase the downward seismic wave energy. The charges that are horizontally distributed with 1 m interval can enhance the seismic wave resolution excited by explosive source. The research shows that the established theoretical model can correctly describe the amplitude-frequency characteristics of the seismic wave field excited by horizontally distributed charges.

1. Introduction

Explosive is the main seismic source that excites the seismic waves artificially in oil and gas prospecting. Gas with high temperature and high pressure would be produced at the moment of explosion and act directly on the geomaterial, resulting in severe damage and forming the blasting cavity in the areas adjacent to the explosive area. With the development of blast wave, the overpressure value drops rapidly till below the failure strength of geomaterial, forming seismic wave in geomaterial [1–6]. Among the above, the explosive source properties can affect the size and acting time of gas detonation pressure; and, as a matter of fact, different types of explosives can form different blasting cavities. In addition, the shape of the charge can also affect the geometrical shape of the blasting cavity. Since the properties of the detonation cavity determine the characteristics of the seismic waves, it can be deemed that the explosive source has significant impacts on the characteristics of seismic waves.

To study the process in which the explosive source forms seismic waves, Jeffreys was the first to establish a cavity vibration model in one-dimensional space, answering questions about full space cavity under spherical pulse [7]. Sharpe studies the wavelets generated by explosion in a closed spherical space, through which he obtained the analytical solution of the pressure elastic wave on the wall of blasting cavity [8]. Targeting at the point-source explosion theoretical model, Blake obtained the analytical solution of elastic waves of non-Poisson body based on Sharpe's study results [9]. Xiao, based on the spreading characteristics of spherical waves in isotropic medium, obtained the amplitude and waveform of spherical waves produced by explosive source [10, 11]. Ding and Zhen studied blasting vibration by equivalent load model and found that the theoretical results are in line with the actual situation [12]; Lin and Bai obtained the pressure solution in the blasting cavity according to the explosion process of explosives in rock and soil [13]. The spherical cavity source models can establish the relationship between the explosion pressure and elastic cavity radius with the seismic wave field. Since these methods simplify the process of explosive source exciting the seismic waves, they cannot build up the direct relationship between the explosive source characteristics and the amplitude-frequency characteristics of seismic wave field. Targeting at this problem,

Yu et al. developed a cavity source model and established the theoretical model for the process in which explosive source excites seismic wave field [14]. This method describes how the explosive source forms the seismic waves, sets up the relationship between initial parameters of explosive source and seismic wave field, and is able to describe the full-field seismic wave characteristics of spherical charge.

Although the seismic source model of spherical cavity can describe the formation and changes of the seismic wave field excited by explosive blasting, multiple sections of cylindrical charges would be adopted as seismic sources. Since the characteristics of the seismic wave field generated by spherical charge and cylindrical charge are different, the traditional seismic source model of spherical cavity is not suitable for describing the seismic wave field produced by cylindrical charge. Heelan analyzed the seismic wavelet excited by finite-length cylindrical charge and obtained the far-field solution of the seismic wave excited by cylindrical charge [15]. As for this method, the detonation pressure at the time of explosive blasting was applied on the excitation medium along the length direction of the cylindrical charge. It directly solves the seismic wave field formed by infinite-length cylindrical charge but cannot describe the seismic wave field characteristics excited by finite-length cylindrical charge. Starfield and Pugliese deemed the cylindrical charge as superposition of multiple short cylindrical charges, thus to solve the blasting stress field at the end of the cylindrical charge when the explosion happens. The calculation results were basically in line with the experimental testing results [16]. Long et al. obtained the development process of the cavity machine formed by cylindrical charge by means of experiment and numerical simulation [17]. On the basis of Yu's results, Li et al. proposed the seismic wave field model of finite-length cylindrical charge by superposition of spherical charges [18, 19]. Hu et al., based on the theory of elastic wave propagation, obtained the relation between the seismic wave field of delayed source and the type of charge, quantity of charge, and interval of charge column by field experiment [20]. Huang et al. figured out the impacts of delayed time of cylindrical charge on seismic wave field from their experimental study conducted on cylindrical charge [21]. However, the above methods are usually used to study the seismic wave characteristics formed by distributive charges through experiments or numerical simulation methods and cannot clearly describe the theoretical relations between horizontally distributed charges and seismic wave field. In order to achieve refined prospecting and control seismic wave characteristics by adjusting the explosive source excitation plan, it is necessary to establish the model for horizontally distributed charges exciting seismic wave field.

In this paper, the whole process in which the explosive source excites the seismic waves was analyzed and the different stages of seismic wave field excited by explosive source were summarized firstly. Considering the spatial structure of the charge, a method for calculating the seismic wave field excited by the horizontally distributed charged was proposed. Meanwhile, on-site experiment was carried out to verify the applicability of this calculation model and further analyze the evolution process in which the horizontally distributed charges excite and form the seismic wave field.

2. Analysis on Process of Explosive Source Exciting Seismic Waves

The process of explosives from blasting to finally forming elastic waves in the distance is accompanied by a series of chemical and physical changes. The energy keeps attenuating during the transmission process due to various dissipation mechanisms, showing the evolution from the powerful blast waves to elastic waves finally. This process is composed of four stages: hydrodynamic stage, geomaterial crushing stage, dynamic expansion stage, and elastic wave propagation stage [22–24]. Meanwhile the medium would have irreversible deformation under the strong explosion effects during the attenuation process, so that the geomaterial near the explosive source shows certain fluid properties under the impacts of huge energy. At the moment of explosion, a wave front could be pushed out from inside the explosion cave, which is in a shape the same as the explosive. With the development of the blast wave, its peak stress attenuates rapidly during the outward propagation process until below the ultimate failure strength of the geomaterial. At this moment, the geomaterial turns from fluid stress state to the elastic-plastic stress state; and the attenuation of the stress wave continues until its peak value falls below a certain value, and the geomaterial transforms from the plastic state to the elastic state. In this case, the explosive source forms the explosion cavity area, plastic area, and an elastic area in sequence when it blasts in geomaterial along the energy transformation direction. However, due to the geometrical difference between the cylindrical charge and the horizontally distributed charge, the development processes of these areas vary to some certain extent: the nearby areas of the cylindrical charge are similar to the shape of the charge, but, with the increase of distance from explosive source, the seismic wave fields excited by cylindrical charge are similar to those excited by distributed charges; and the seismic wave field excited by distributed charge develops from ellipsoid to a spherical shape gradually till forming wave front similar to that of the cylindrical charge. For the comparison of area shapes, see Figure 1.

3. Model for Seismic Wave Field Excited by Spherical Explosive

The model of spherical cavity seismic source can be used to describe the relationship between the explosive source and the seismic wave field. In this model, large amounts of gases with high temperature and high pressure generated at the moment of blasting act directly on the geomaterials and form blasting cavity. Since the gas pressure inside the cavity is far greater than the geomaterial strength, the geomaterial near the explosives shows fluid property under huge pressure, so that the blasting cavity can be deemed as expanding in incompressible flow. With the propagation and

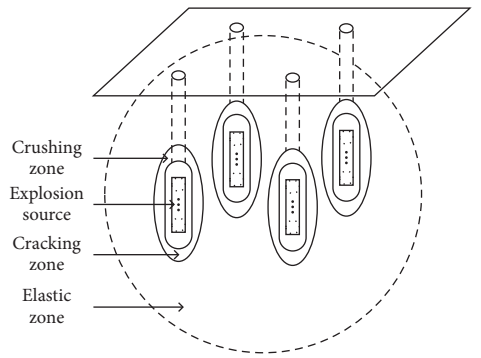

Figure 1: Explosive zoning of horizontally distributed charge in geomaterial.

attenuation of blast waves in medium, the blast waves keep attenuating till below the medium failure strength at place which is certain distance away from the explosive source. At this time, the excitation medium shows elastic properties. Yu supposed that the detonation process and blast cavity are formed instantaneously. Then, under the condition that the soil medium is incompressible and the property change is ignored, a quasi-static model for predicting the blast cavity of the spherical charge was established, through which the blast cavity radius and the plastic zone radius excited by the spherical charge in geomaterial can be obtained.

Radius of blast cavity is

$$b_* = a_0\left(\frac{P_0}{-(c/\varphi)+(\sigma_*+(c/\varphi))L^{(4f/3(1+f))}}\right)^{(1/3\gamma)}\sqrt[3]{\frac{2\mu}{3\sigma_*}}, \tag{1}$$

where

$$L = \frac{\mu}{\sigma_*\left[1+\ln\left(\sigma_*/\sigma_0\right)\right]}. \tag{2}$$

Radius of plastic zone is

$$b_0 = \left(\frac{\sigma_*}{\sigma_0}\right)^{(1/2)} b_*, \tag{3}$$

where a_0 is the spherical charge radius, P_0 is the initial blasting pressure of the explosive, γ is the explosive expansion index, φ is the cohesion of the soil medium, c is the internal friction angle of soil medium, σ_* is the compressive strength of the soil medium, σ_0 is the tensile strength of the soil medium, and μ is the lame coefficient (shearing modulus in elastic medium).

The linear radial strain and hoop strain are introduced according to the spherical symmetry and linear theory to simplify the motion equation as follows:

$$\frac{\partial^2 u}{\partial r^2}+\frac{2}{r}\frac{\partial u}{\partial r}-2\frac{u}{r^2}=\frac{1}{c^2}\frac{\partial^2 u}{\partial t^2}. \tag{4}$$

The solution of this equation can describe the forced vibration of the particle under viscous damping, and its general form is

$$U(r,t) = e^{-\left(\eta^2\tau/\rho_{\text{soil}}cb_*\right)}\left[\left(\frac{Pb_*^2c}{\eta\kappa r^2}-\frac{\eta Pb_*}{\kappa\rho_{\text{soil}}cr}\right)\sin\frac{\eta\kappa\tau}{\rho_{\text{soil}}cb_0}+\frac{Pb_*}{\rho_{\text{soil}}cr}\cos\frac{\eta\kappa\tau}{\rho_{\text{soil}}cb_0}\right], \tag{5}$$

where

$$\begin{aligned}\eta^2 &= \frac{2(1-2\sigma)\rho_{\text{soil}}c^2+3(1-\sigma)\gamma P}{2(1-\sigma)},\\ \kappa^2 &= \frac{2\rho_{\text{soil}}c^2-3(1-\sigma)\gamma P}{2(1-\sigma)},\\ \tau &= t-\frac{r-b_0}{c}.\end{aligned} \tag{6}$$

The main frequency of vibration in the above equation can be expressed as

$$\begin{aligned}f_1 &= \frac{\omega}{2\pi}\\ &= \frac{\eta\kappa}{2\pi\rho_{\text{soil}}cb_0}\\ &= \frac{\sqrt{\left(8\rho_{\text{soil}}c^2-9\gamma P\right)\left(4\rho_{\text{soil}}c^2+9\gamma P\right)}}{12\pi\rho_{\text{soil}}cb_0}.\end{aligned} \tag{7}$$

Vibration amplitude can be expressed as

$$A_0 = e^{-\left(\eta^2T/\rho_{\text{soil}}cb_0\right)}\frac{P}{\eta\kappa}\frac{b_0^2}{2\rho_{\text{soil}}c^2r}. \tag{8}$$

4. Method to Calculate Seismic Wave Field Excited by Horizontally Distributed Charges

The horizontally distributed charge is composed of cylindrical charges with equal lengths arranged at equal intervals along the axial direction of the cylindrical charge. Supposing that each cylindrical charge is equivalent to the superposition of multiple spherical charges, the horizontally distributed charge can be regarded as a multilevel continuous spherical charges superimposed at intervals. Since different sections of cylindrical charges are of different spatial positions, different spherical equivalent charges have different positions relative to a certain point in the space, and vibration directions of designated positions excited by each charge are different, we need to decompose the vibration resulting by each spherical charge. Then, we should superimpose, respectively, at x-direction, y-direction, and z-direction to finally obtain the resultant velocity. However, each section of cylindrical charge shall satisfy the following conditions: (1) The total volume of the charge is equal to the total volume of all spherical charges. (2) The total length of the charge is equal to the sum of the diameters of all spherical charges. (3) The continuity of the detonation process and the equivalent spherical charge interval of all sections of cylindrical charges shall be zero.

As shown in Figure 2, the vibration velocity of the seismic wave excited by No. n spherical equivalent explosive in No. m section at point A in the space should be $U_{mn}(r,t)$, the velocity component in the x-direction should be $U_{mnx}(r,t)$, the velocity component in the y-direction should be $U_{mny}(r,t)$, and the velocity component in the z-direction should be $U_{mnz}(r,t)$; then

$$U_{mnx}(r,t) = U_{mn}(r,t)\frac{L_{mnx}}{r_{mn}},$$

$$U_{mny}(r,t) = U_{mn}(r,t)\frac{L_{mny}}{r_{mn}}, \tag{9}$$

$$U_{mnz}(r,t) = U_{mn}(r,t)\frac{L_{mnz}}{r_{mn}},$$

where L_{mnx}, L_{mny}, and L_{mnz} are the distances between No. n spherical equivalent charge in No. m section and point A in three directions; r_{mn} is the actual distance between No. n spherical equivalent charge in No. m section and point A in three directions.

Then the velocity components of vibration velocity of No. m section of cylindrical charge at point A in x-direction, y-direction, and z-direction, namely, $U_{mx}(r,t)$, $U_{my}(r,t)$, and $U_{mnz}(r,t)$, are, respectively,

$$\begin{aligned} U_{mx}(r,t) &= U_{m1x}(r,t) + U_{m2x}(r,t) + \cdots + U_{mnx}(r,t),\\ U_{my}(r,t) &= U_{m1y}(r,t) + U_{m2y}(r,t) + \cdots + U_{mny}(r,t),\\ U_{mz}(r,t) &= U_{m1z}(r,t) + U_{m2z}(r,t) + \cdots + U_{mnz}(r,t). \end{aligned} \tag{10}$$

Then the velocity components of vibration velocity of the whole horizontally distributed charge at point A in x-direction, y-direction, and z-direction, namely, $U_x(r,t)$, $U_y(r,t)$, $U_z(r,t)$, are, respectively,

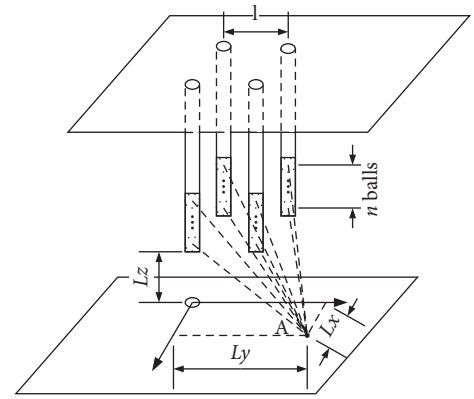

Figure 2: Horizontally distributed excitation scheme.

$$\begin{aligned} U_x(r,t) &= U_{1x}(r,t) + U_{2x}(r,t) + \cdots + U_{mx}(r,t),\\ U_y(r,t) &= U_{1y}(r,t) + U_{2y}(r,t) + \cdots + U_{my}(r,t),\\ U_z(r,t) &= U_{1z}(r,t) + U_{2z}(r,t) + \cdots + U_{mz}(r,t). \end{aligned} \tag{11}$$

Then the resultant velocity is

$$U(r,t) = \sqrt[3]{U_x(r,t)^3 + U_y(r,t)^3 + U_z(r,t)^3}. \tag{12}$$

The amplitude-frequency characteristics of the seismic waves excited by the horizontally distributed charge are closely related to the interval between all charges. Proper interval could produce greater energy. By overlapping the peak pressure of blast wave excited by the first section of cylindrical charge to the peak value of blast wave excited by the second section of cylindrical charge, we could obtain the best superposition effects.

5. Verification of the Model for Seismic Wave Field Excited by Horizontally Distributed Charges

Due to the special geometric structure of the horizontally distributed charges, the seismic waves that it excites in the soil vary in horizontal and vertical directions. In the area near the charge, stress wave front will spread outwards based on the basic shape of each section of the charge. With the geometric divergence and the propagation of seismic waves in the soil, seismic waves show different characteristics in the horizontal and vertical directions. In order to verify the effectiveness of the method for calculating the seismic wave field excited by the horizontally distributed charge, three different excitation schemes were applied in this study to make comparison on the theoretical calculation results and the numerical simulation results of the seismic wave field excited by the horizontally distributed charge in the axial and radial directions. For the detailed excitation parameters, please see Table 1.

The results calculated by the theoretical model are compared with the results obtained by the finite element

Table 1: Excitation scheme of axially distributed explosives.

SN	No. of cylindrical charges	Mass of each section of cylindrical charge (kg)	Interval between cylindrical charges (m)	Total charges (kg)	Delayed time (s)	Excitation direction
1	4	1	0.03	4	0	Top
2	4	1	1	4	0	Top
3	4	1	2	4	0	Top

software Autodyn, among which the soil medium parameters and TNT explosive characteristic parameters are shown in Tables 2 and 3.

The standard JWL equation for ideal detonation products was adopted as the TNT state equation:

$$P = C_1\left(1 - \frac{\omega}{r_1 v}\right)e^{-r_1 v} + C_2\left(1 - \frac{\omega}{r_2 v}\right)e^{-r_2 v} + \frac{\omega e}{v}, \quad (13)$$

where e is the detonation energy, and C_1, C_2, R_1, R_2, and ω are the parameters of state equation; please see Table 3.

Ideal elastic-plastic model was applied for soil medium. The state equation is

$$P = k\mu, \quad (14)$$

where $\mu = (\rho/\rho_0) - 1$ and k is the bulk modulus.

von Mises strength model was applied as the strength model of soil medium:

$$(\sigma_1 - \sigma_2)^2 + (\sigma_2 - \sigma_3)^2 + (\sigma_3 - \sigma_1)^2 = 2\sigma_s^2 = 6G^2, \quad (15)$$

where σ_s is yield strength, G is the shearing modulus, and the parameters shown in Table 2 were used for soil medium.

To analyze the functions of distributed seismic sources, three types of calculation models were established targeting at the centralized 4 kg charge, 4×1 kg charge (1 m × 1 m), and 4×1 kg charge (2 m × 2 m), respectively, for conducting comparative analysis on their theoretical calculation results and numerical simulation calculating results. Figure 3 shows three types of charges on a same plane. Figure 3(a) is the centralized charge, Figure 3(b) shows charges with 1 m interval, and Figure 3(c) shows charges with 2 m interval.

Figure 4 shows the changes of soil plastic deformation due to impact pressure in scheme I (centralized). Explosives explode in the soil and produce shock waves that travel outwards in a cylindrical shape. The plastic deformation area of the soil is also cylindrical. It appears as a ring on a horizontal section, the plastic deformation area increases gradually with time, and there is a volume upper limit.

Figure 5 shows the changes of soil plastic deformation due to impact pressure in scheme II (1 m × 1 m). Every explosive charge explodes in the soil and produces shock waves that travel outwards in a cylindrical shape. The plastic deformation area of the soil is also cylindrical, and it appears as a ring on a horizontal section. The plastic deformation area increases with time. When $t = 0.8$ ms, the plastic area around the adjacent gun holes is connected. When $t = 1.4$ ms, all the soils between the 4 holes are plastically deformed. When the shock wave passes completely, the soil is unloaded and its properties are restored to an elastic state, but the elastic state is different from the initial state.

Figure 6 shows the changes of soil plastic deformation due to impact pressure in scheme III (2 m × 2 m). Every explosive charge explodes in the soil and produces shock waves that travel outwards in a cylindrical shape. The plastic deformation area of the soil is also cylindrical, and it appears as a ring on a horizontal section. When $t = 0.8$ ms, the plastic deformation area increases with time. The plastic area reaches its maximum volume when $t = 1.2$ ms. When the shock wave passes completely, the soil is unloaded and its properties are restored to an elastic state, but the elastic state is different from the initial state.

The explosives in scheme I (Centralized) explode in the soil to produce the smallest area of plastic deformation. The plastic deformation areas of the explosives in schemes II (1 m × 1 m) and III (2 m × 2 m) are approximately equal at the initial moment ($t < 0.8$ ms) when they explode in the soil. However, due to the closer distance between the explosives in scheme II (1 m × 1 m), in the moment (8 ms < t < 14 ms), the area of soil deformation near the center part of the area is smaller, which causes the plastic deformation of the moment scheme II (1 m × 1 m) to be smaller than the area of scheme III (2 m × 2 m).

Figure 7 shows the comparison between the theoretical calculation results and the numerical simulation results of the maximum vibration velocity of the seismic waves excited by three different excitation schemes. As for the comparison of the maximum vibration velocities calculated based on theory and numerical simulation at the places with the same distance to explosive center, in horizontal direction, significant errors appear when the central axis horizontal distance is within 5 m, reaching about 3%–7%; the error between the two decreases with the increase of distance to explosive center. When the distance of shaft centers enlarges to over 8 m, the error would be within 3%. On the vertical direction of the central axis, the error between the two is within 5%. It can be figured out that the two values vary greatly on horizontal direction. That is because the end effects when the equivalent spherical vibrations are superimposed on the horizontal direction lead to greater theoretical calculation result. With the increase of distance to explosive center, the effect of the geometric structure decreases gradually, so that the gap at farther distances gradually decreases.

Distributed charges can effectively reduce the impacts on ground vibration. The greater the interval between charges, the more significant the shock absorption effect. This is mainly because when the charges are arranged close to each other, the blasting cavities that the charges formed at the time of detonation would be superimposed, which increases the disturbance to the ground. With the increase of the

Table 2: Parameters of soil.

σ_* (MPa)	σ_0 (MPa)	μ (GPa)	c	φ (kPa)	ρ_{soil} (kg · m^3)	K (MPa)	G (MPa)	σ_s (MPa)
13	2	0.147	0.115	11.8	1840	245	147	22

Table 3: Parameters of TNT.

C_1(GPa)	C_2 (GPa)	R_1	R_2	ω	ρ(kg · m^{-3})	D (m · s^{-1})	E (J · m^{-3})	P_{CJ} (GPa)	P_0 (GPa)
373.7	3.747	4.15	0.90	0.35	1650	6930	6.0×10^9	21	9.82

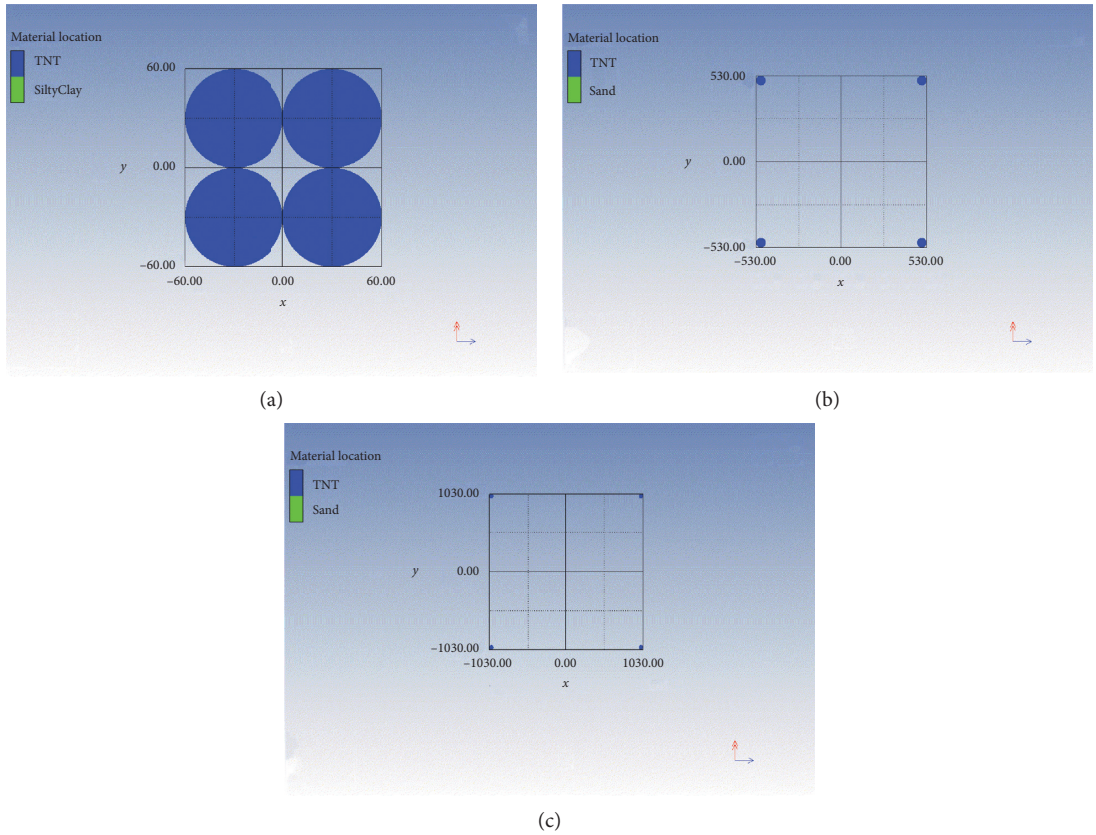

Figure 3: Charges with different intervals on the same plane (observed at depth of $z = -1$ m). (a) Centralized charge. (b) Charge with 1 m interval. (c) Charge with 2 m interval.

interval, the plastic zones formed by the charges are separated, which reduces the disturbance to the ground. Besides, the distributed charge can effectively improve the vibration velocity of downward propagation. Such phenomenon is also related to the interval between charges. When applying proper interval, the downward-propagated seismic waves excited by the charges would also be superimposed, thereby increasing the amplitude of the seismic wave.

6. Discussion

The geometric structure of the horizontally distributed charge determines that the characteristics of the seismic wave field in area near the explosive source are different at the axial direction and the radial direction. In order to study the development status of the seismic wave field excited by the horizontally distributed charges, the seismic wave fields at the vertical and horizontal directions of the central axis of the centralized charge and the horizontally distributed charge were studied in this paper; and, for the three conditions of centralized charge, charges with 1 m interval, and charges with 2 m interval, their seismic wave amplitude-frequency characteristics at places 12 m away from central axis along both the vertical and horizontal directions were solved according to the spherical-cylindrical conversion model (Figure 8).

At the place with 12 m distance along the horizontal direction, the maximum vibration velocities of the centralized charge, charges with 1 m interval, and charges with 2 m interval are, respectively, 0.20 m/s, 0.15 m/s, and 0.05 m/s, the main frequencies are 125 Hz, 105 Hz, and 55 Hz, and the frequency bandwidths are 120 Hz, 95 Hz, and 48 Hz, respectively. The seismic waves excited by centralized charge are greater than those formed by distributed charges

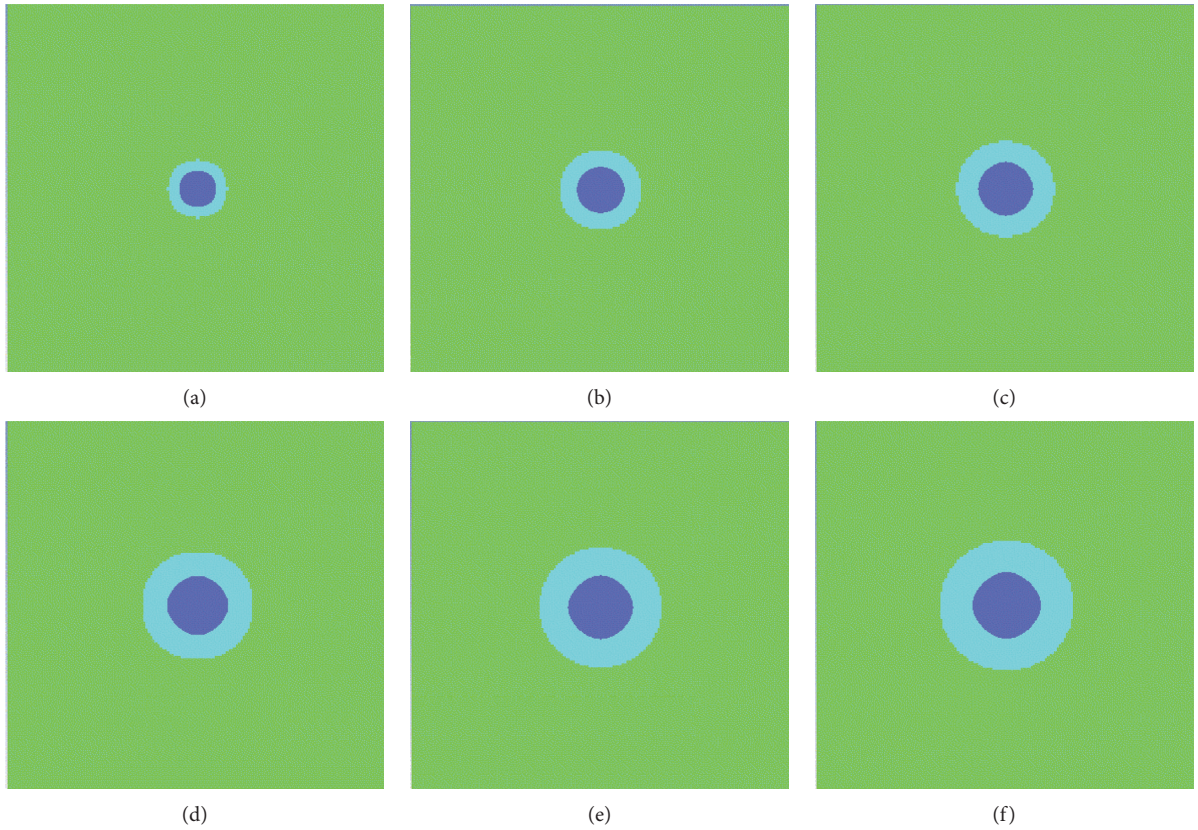

Figure 4: A diagram of soil plasticity changes in the horizontal cross section of explosive explosion in scheme I (centralized). (a) 0.2 ms, (b) 0.4 ms, (c) 0.6 ms, (d) 0.8 ms, (e) 1.0 ms, and (f) 1.2 ms.

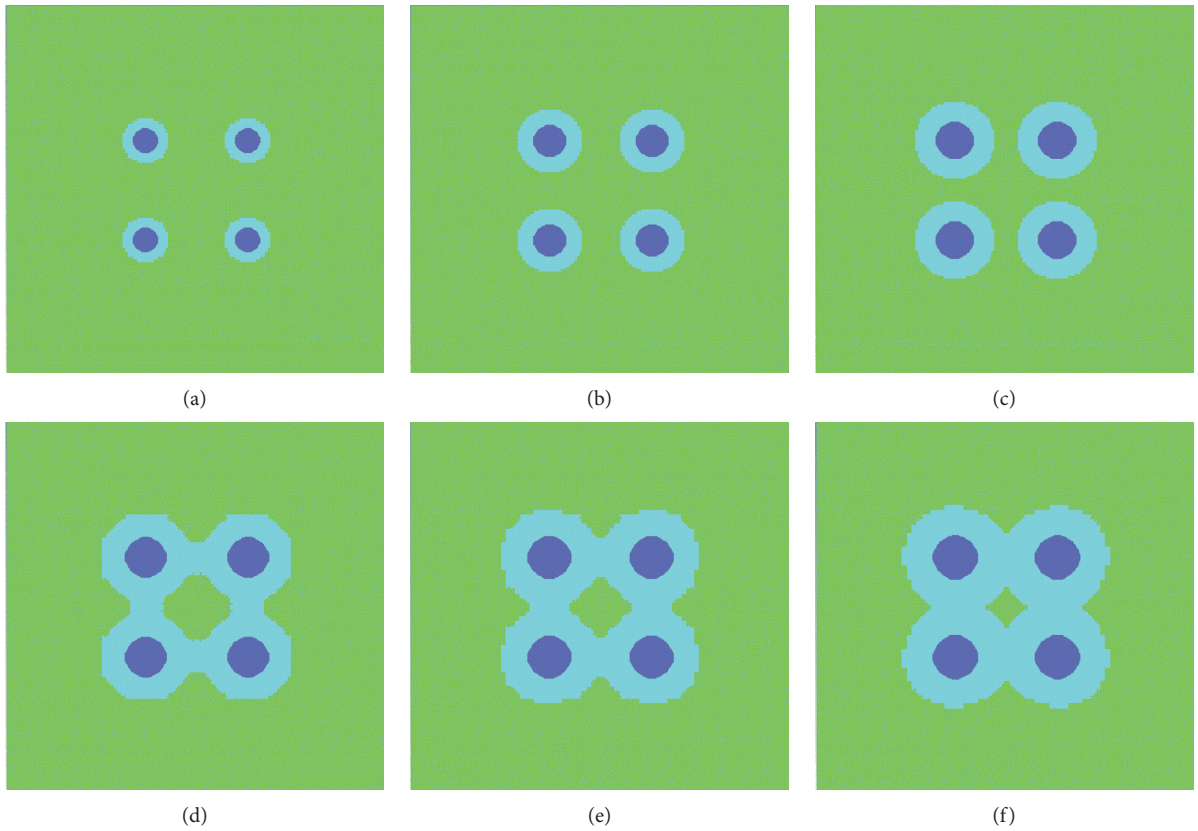

Figure 5: A diagram of soil plasticity changes in the horizontal cross section of explosive explosion in scheme II (1 m × 1 m). (a) 0.2 ms, (b) 0.4 ms, (c) 0.6 ms, (d) 0.8 ms, (e) 1.0 ms, and (f) 1.2 ms.

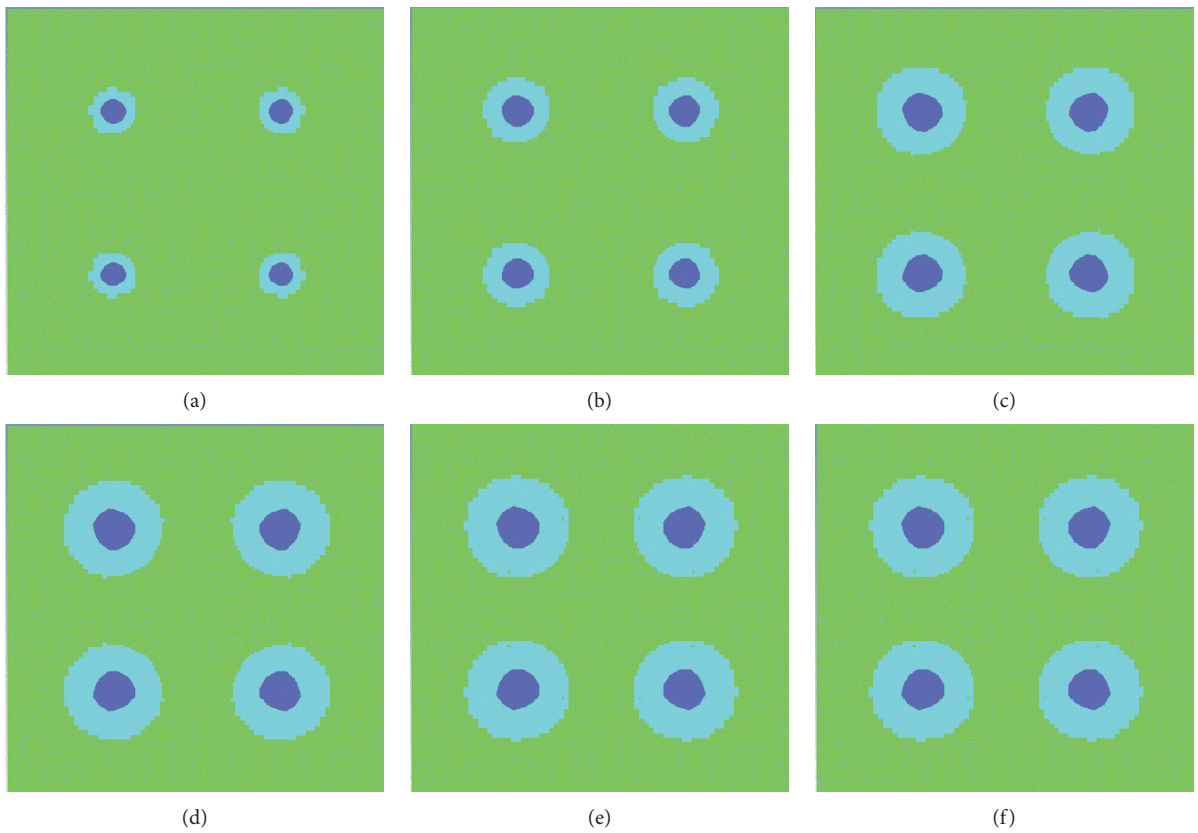

Figure 6: A diagram of soil plasticity changes in the horizontal cross section of explosive explosion in scheme III (2 m × 2 m). (a) 0.2 ms, (b) 0.4 ms, (c) 0.6 ms, (d) 0.8 ms, (e) 1.0 ms, and (f) 1.2 ms.

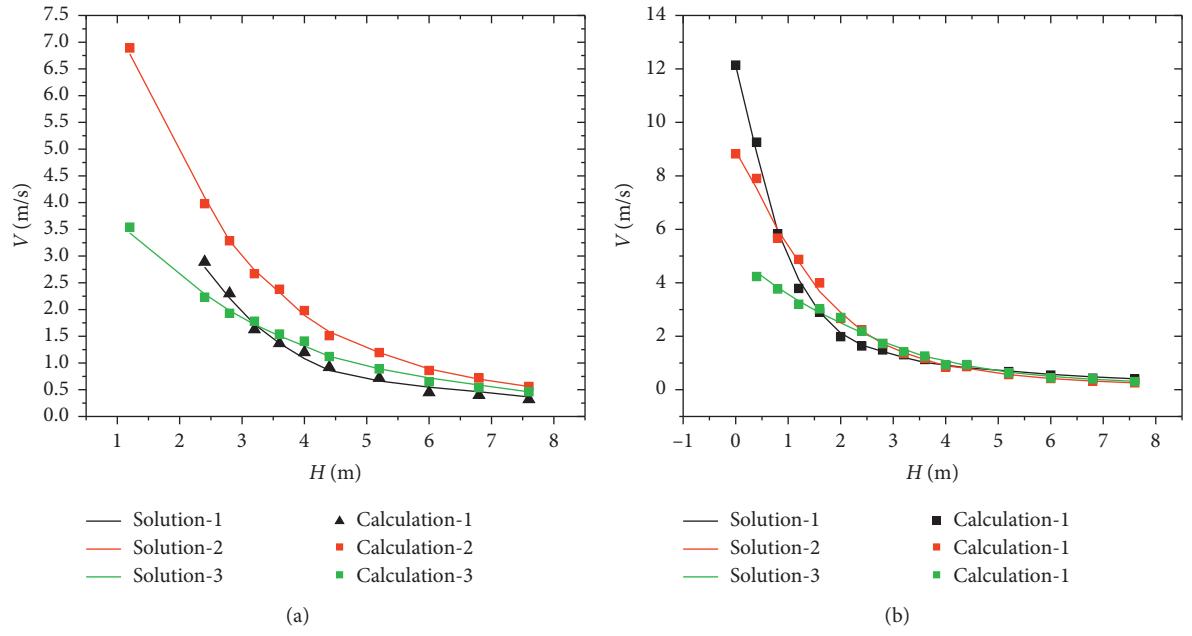

Figure 7: Comparison on max. vibration velocity of different excitation schemes.

in both the energy and frequency. The energy and frequency of seismic waves formed by charges with 2 m interval are both greater than those formed by charges with 1 m interval. The main reason is that the seismic wave time difference resulting by charge interval on horizontal direction makes the peak value zones of seismic waves formed by all equivalent charges unable to be superimposed, so that "the greater the charge interval, the lower the max. vibration

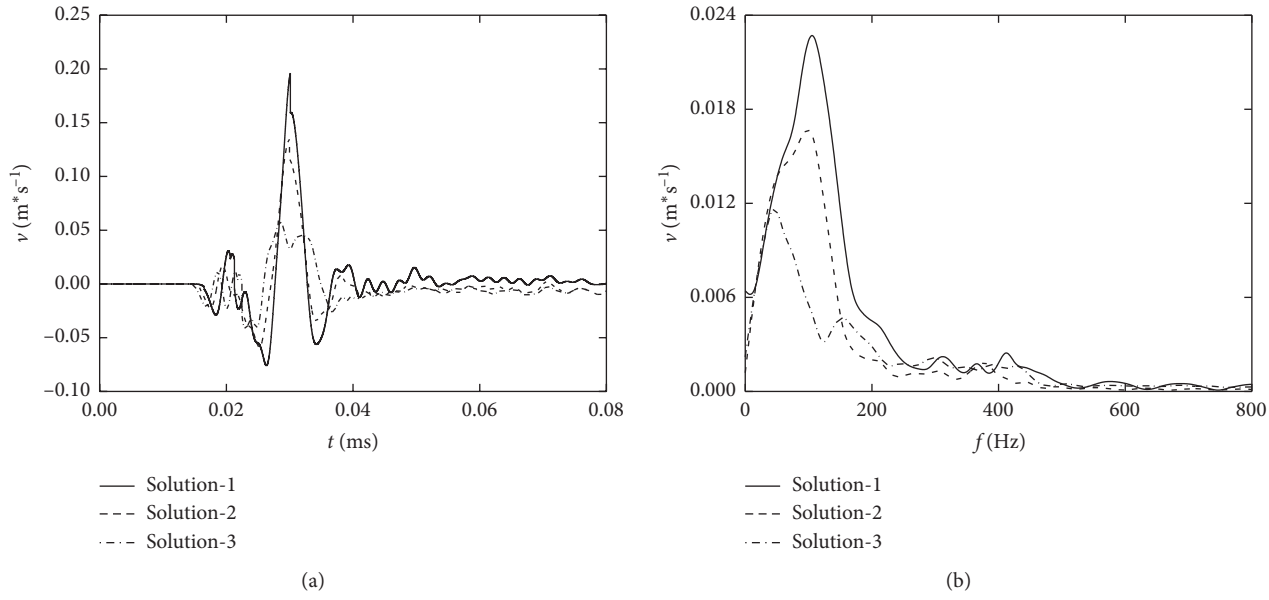

Figure 8: Waveform and frequency at place 12 m away from the central position at horizontal direction.

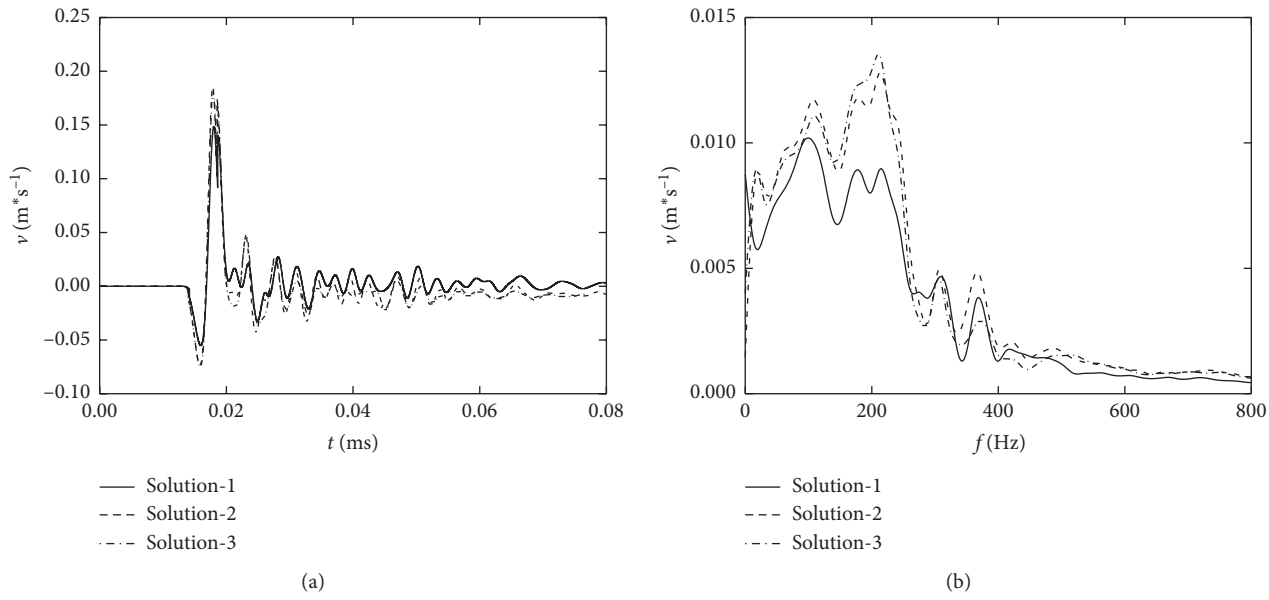

Figure 9: Waveform and frequency at place 12 m away from the central position at vertical direction.

velocity of the seismic wave"; and, in the transverse direction, the radius of the plastic zone formed by centralized charge must be smaller than that formed by distributed charges. With the increase of the charge interval, the sum of the plastic zones would be increased. Therefore, the greater the charge interval, the lower the frequency of the seismic wave (Figure 9).

At the place 12 m away along vertical direction, the maximum vibration velocities of the centralized charge, charges with 1 m interval, and charges with 2 m interval are, respectively, 0.15 m/s, 0.17 m/s, and 0.19 m/s, the main frequencies are 105 Hz, 125 Hz, and 120 Hz, and the bandwidths are 100 Hz, 125 Hz, and 122 Hz, respectively. It can be found that the energy and frequency of the seismic wave formed by the centralized charge are less than the energy and frequency of the seismic wave formed by the distributed charge. The energy and frequency of the seismic wave excited by charges with 2 m interval are less than those that formed the distributed charge with 1 m interval. The reason for this phenomenon is that the radius of the plastic zone that formed along the vertical direction when the charge is exploded will not deviate due to the difference of the distribution of the charges. The time difference caused by the interval between the cylindrical charges will still affect the superposition of the peak vibration velocities of the seismic waves, so as to lead to different peak value vibration velocities formed by distributed charges.

7. Conclusions

To clarify the relationship between the horizontally distributed cylindrical charge and the seismic wave field, the spherical cavity seismic source model was taken as the basis, and the method of replacing cylindrical charges by equivalent superposition of multiple spherical charges was applied to propose the approach of calculating the seismic wave field excited by horizontally distributed charges and establish the model for seismic wave field excited by horizontally distributed charges. Traditional models for spherical charge explosive source and the cylindrical charge explosive source cannot accurately describe the seismic wave field characteristics excited by distributed charges during seismic prospecting. But the model proposed in this paper overcomes this setback and provides theoretical basis for conducting the refined prospecting and production.

Two methods of numerical simulation and on-site test were applied to verify the applicability of the theoretical model. The results of the numerical simulation calculation show that, in the radial direction, the error of calculation results between the theoretical model and the numerical model is within 7%; and, along the horizontal direction, the error of calculation results between the theoretical model and the numerical model is within 3.4%. This indicates that the distributed charges can effectively reduce the impact of ground vibration and increase the energy of seismic waves propagating downwards.

At the detonation moment of the horizontally distributed charge, the seismic wave fields formed near the explosive show differences along horizontal and vertical directions. Under the condition of the same horizontal distance, the vibration velocity along the horizontal direction reduces with the increase of explosive interval. When the horizontal distance is set to be 12 m, the maximum vibration velocity of the centralized charges, charges with 1 m interval, and charges with 2 m intervals would be 0.20 m/s, 0.15 m/s, and 0.05 m/s, respectively, the main frequencies are 125 Hz, 105 Hz, and 55 Hz, and the bandwidths are 120 Hz, 95 Hz, and 48 Hz. When the vertical distance is set to be 12 m, the maximum vibration velocity of the centralized charges, the charges with 1 m interval, and the charges with 2 m interval would be 0.15 m/s, 0.17 m/s, and 0.19 m/s, respectively, the main frequencies are 105 Hz, 125 Hz, and 120 Hz, and the bandwidths are 100 Hz, 125 Hz, and 122 Hz, respectively. The results show that the horizontally distributed charges with 2 m interval are the most satisfactory choice to achieve the goal of improving explosive source seismic wave resolution by adjusting the excitation form of explosive source.

Data Availability

The data are available and included within this article; readers can access the data supporting the conclusions of this study.

Conflicts of Interest

The authors declare that there are no conflicts of interest.

Authors' Contributions

The manuscript was approved by all authors for publication.

Acknowledgments

The authors would like to acknowledge the State Key Laboratory of Explosion Science and Technology at Beijing Institute of Technology. This work was supported by the National Natural Science Foundation of China (no. 51678050) and the National Key R&D Program of China (no. 2017YFC0804702).

References

[1] Y. Wang, W. K. Feng, R. L. Hu, and C. H. Li, "Fracture evolution and energy characteristics during marble failure under triaxial fatigue cyclic and confining pressure unloading (FC-CPU) conditions," *Rock Mechanics and Rock Engineering*, vol. 54, no. 2, pp. 799–818, 2021.

[2] Z. G. Tao, C. Zhu, M. C. He et al., "A physical modeling-based study on the control mechanisms of negative Poisson's ratio anchor cable on the stratified toppling deformation of anti-inclined slopes," *International Journal of Rock Mechanics and Mining Sciences*, vol. 138, p. 104632, 2021.

[3] C. Zhu, M. He, M. Karakus, X. Zhang, and Z. Tao, "Numerical simulations of the failure process of anaclinal slope physical model and control mechanism of negative Poisson's ratio cable," *Bulletin of Engineering Geology and the Environment*, vol. 80, no. 4, pp. 3365–3380, 2021.

[4] B. Li, R. Bao, Y. Wang, and C. Zhao, "Permeability evolution of two-dimensional fracture networks during shear under constant normal stiffness boundary conditions," *Rock Mechanics and Rock Engineering*, vol. 54, no. 3, pp. 1–20, 2021.

[5] Q. Wang, H. K. Gao, B. Jiang, S. Li, M. He, and Q. Qin, "In-situ test and bolt-grouting design evaluation method of underground engineering based on digital drilling," *International Journal of Rock Mechanics and Mining Sciences*, vol. 138, Article ID 104575, 2021.

[6] Q. Wang, Q. Qin, B. Jiang et al., "Mechanized construction of fabricated arches for large-diameter tunnels," *Automation in Construction*, vol. 124, Article ID 103583, 2021.

[7] H. Jeffreys, "On the cause of oscillatory movement in seismograms," *Geophysical Journal International*, vol. 2, no. 2, pp. 407–416, 1931.

[8] J. A Sharpe, "The production of elastic waves by explosion pressure. I. Theory and empirical field observations," *Geophysics*, vol. 2, no. 7, pp. 144–154, 1942.

[9] F. G. Blake, "Spherical wave propagation in solid media," *The Journal of the Acoustical Society of America*, vol. 2, no. 24, p. 211, 1952.

[10] J. H. Xiao and W. T. Sun, "Seismic wavelet generated by point explosive source," *Oil Geophysical Prospecting*, vol. 6, no. 32, pp. 809–817, 1997.

[11] J. H. Xiao, "Argument on wave equation of spherical wave," *Oil Geophysical Prospecting*, vol. 2, no. 36, pp. 160–172, 2001.

[12] H. Ding and Z. M. Zhen, "Blasting vibration equivalent load model," *Scientia Sinica Techologica*, vol. 1, no. 33, pp. 82–90, 2003.

[13] D. C. Lin and C. H. Bai, *The Effect of Explosion Earthquakes*, Geological Publishing House, Beijing, China, 2007.

[14] C. L. Yu, Z. Q. Wang, and W. G. Han, "A prediction model for amplitude-frequency characteristics of blast-induced seismic

waves," *Geophysics: Journal of the Society of Exploration Geophysicists*, vol. 83, no. 3, pp. 1–56, 2018.

[15] P. A. Heelan, "Radiation from a cylindrical source of finite length," *Geophysics*, vol. 18, no. 3, pp. 685–696, 1953.

[16] A. M. Starfield and J. M. Pugliese, "Compression waves generated in rock by cylindrical explosive charges: a comparison between a computer model and field measurements," *International Journal of Rock Mechanics and Mining Sciences & Geomechanics Abstracts*, vol. 1, no. 5, pp. 65–77, 1968.

[17] Y. Long, X. S. Lin, and L. P. Xu, "Experimental research on growth process of the cavity of a strip-shaped explosive charge exploding in soil," *Explosion and Shock Waves*, vol. 3, pp. 227–235, 1988.

[18] P. Y. Li, Z. Q. Wang, and Q. Xu, "Calculation method for characteristic size of blasting cavity of finite length cylindrical charges in soil," *Explosion and Shock Waves*, vol. 12, no. 39, pp. 100–108, 2019.

[19] C. L. Yu and Z. Q. Wang, "Quasi-static model for predicting explosion cavity with spherical charges," *Explosion and Shock Waves*, vol. 2, no. 37, pp. 249–254, 2017.

[20] L. X. Hu, D. K. Yang, B. S. He et al., "Theoretic analysis of delayed blast," *Oil Geophysical Prospecting*, vol. 1, no. 37, pp. 33–38, 2002.

[21] W. Y. Huang, S. L. Yan, S. R. Lv et al., "The research and application of the low detonation velocity and elongated source charge," *Explosive Materials*, vol. 4, pp. 18–22, 2005.

[22] X. J. Yang, J. M. Wang, C. Zhu, M. C. He, and Y. Gao, "Effect of wetting and drying cycles on microstructure of rock based on SEM," *Environmental Earth Sciences*, vol. 78, no. 6, p. 183, 2018.

[23] L. Ban, C. Zhu, C. Qi, and Z. Tao, "New roughness parameters for 3D roughness of rock joints," *Bulletin of Engineering Geology and the Environment*, vol. 78, no. 6, pp. 4505–4517, 2019.

[24] A. Li, F. Dai, Y. Liu et al., "Dynamic stability evaluation of underground cavern sidewalls against flexural toppling considering excavation-induced damage," *Tunnelling and Underground Space Technology*, vol. 112, Article ID 103903, 2021.